Mitigation of bromine-containing products during pyrolysis of polycarbonate-based tetrabromobisphenol A in the presence of copper (I) oxide

Sylwia Oleszek[1,2,*], Shogo Kumagai[3], Mariusz Grabda[2], Kenji Shiota[1], Toshiaki Yoshioka[3], Masaki Takaoka[1]

Authors' affiliations and contact data:

Sylwia Oleszek* **(corresponding author)**

[1]Department of Environmental Engineering, Graduate School of Engineering, Kyoto University, Nishikyo-ku, Katsura C-1-3, 615-8540 Kyoto, Japan.

Telephone: +81-75-383-3335; Fax: +81-75-383-3338

E-mail (1): oleszek.sylwia.2r@kyoto-u.ac.jp

E-mail (2): sylwia_oleszek@yahoo.com

[2] Institute of Environmental Engineering of the Polish Academy of Sciences, M. Sklodowska-Curie 34, 41-819 Zabrze, Poland

Shogo Kumagai

[3]Graduate School of Environmental Studies, Tohoku University, 6-6-07 Aoba, Aramaki-Aza, Aoba-ku, Sendai 980-8579, Japan

E-mail: kumagai@tohoku.ac.jp

Mariusz Grabda

[2] Institute of Environmental Engineering of the Polish Academy of Sciences, M. Sklodowska-Curie 34, 41-819 Zabrze, Poland.

E-mail: mariusz_grabda@icloud.com

Kenji Shiota

[1]Department of Environmental Engineering, Graduate School of Engineering, Kyoto University, Nishikyo-ku, Katsura C-1-3, 615-8540 Kyoto, Japan.

E-mail: shiota.kenji.4x@kyoto-u.ac.jp

Toshiaki Yoshioka

[3]Graduate School of Environmental Studies, Tohoku University, 6-6-07 Aoba, Aramaki-Aza, Aoba-ku, Sendai 980-8579, Japan.

E-mail: yoshioka@tohoku.ac.jp

Masaki Takaoka

[1]Department of Environmental Engineering, Graduate School of Engineering, Kyoto University, Nishikyo-ku, Katsura C-1-3, 615-8540 Kyoto, Japan.

E-mail: takaoka.masaki.4w@kyoto-u.ac.jp

Abstract

Polycarbonate (PC) is an engineering thermoplastic that is widely used in electrical and electronic equipment. This plastic often contains tetrabromobisphenol A (TBBA), the most common brominated flame retardant. Thermal degradation of the PC-TBBA leads to generation of numerous bromo-organic products in the pyrolytic oil, hindering its appropriate utilization, as well as corrosive hydrogen bromide gas. The purpose of this study was to experimentally investigate and compare the pyrolysis products of PC-TBBA and PC-TBBA+Cu_2O at various temperatures, with an emphasis on the yield and distribution of brominated compounds. In pyrolysis of PC-TBBA+Cu_2O, at the maximum degradation temperature (600 °C), as much as 86% of total Br was trapped in the residue, while 3 and 11% were distributed in the condensate and gas fractions, respectively. In contrast, the distribution of Br from non-catalytic pyrolysis of PC-TBBA (600 °C) was 0.5% residue, 40% condensate, and 60% gas. The results of this study revealed that in the presence of Cu_2O, organo-bromine products were most likely involved in Ullman-type coupling reactions, leading to early cross-linking of the polymer network that efficiently hinders their vaporization. HBr in the gas fraction was suppressed due to effective fixation of bromine in residue in the form of CuBr.

Keywords: pyrolysis, bromine distribution, catalytic effect, cross-coupling reactions, fixed bed reactor.

1. Introduction

Waste electrical and electronic equipment (WEEE) is the fastest growing waste stream worldwide. In 2016, global generation of WEEE was 44.7 million metric tons (Mt) and is estimated to grow to more than 52.2 Mt by 2021 (GDFEEW, 2019). WEEE is a highly diverse waste material composed mainly of ferrous and nonferrous metals, along with plastics. Plastics constitute approximately 20–30% of the total WEEE fraction, of which polycarbonate (PC) represents 10% (Kousaiti et al., 2020).

PC manufactured using bisphenol A is the most commonly used engineering thermoplastic in automobiles, electronic devices, batteries, data-recording media, and medical equipment, due to its low weight, high compatibility, durability, and excellent impact resistance (Levchik and Weil, 2005). Global demand for PC was approximately 3.4 Mt in 2010. Due to growing interest in new technologies such as virtual reality devices, sensors, and drones, this demand is expected to grow by 7% per year (Grigorescu et al., 2019). The growing electronics market and increasing consumption of this polymer indicate that a resource-conserving and economically viable recycling process for PC is essential and will offer both economic and environmental benefits. As noted by Chandrasekaran et al., 2018, approximately 2.5 million tons of PC can potentially be recovered from WEEE annually.

Pyrolysis is regarded as an adequate method of WEEE recycling, enabling separation of organic and inorganic matter (Sharrudin et al., 2016; Shen et al., 2016). During pyrolysis (in the absence of oxygen), inorganic matter (metals, fillers) remains unchanged in the solid residue while decomposed organic matter is transferred into three major fractions (char, oil, and gas), which are valuable secondary materials used in diverse industries. The yield and

chemical composition of each fraction depend on the chemical composition of the starting material and the operating parameters of pyrolysis (e.g., temperature, heating rate, pressure, residence time, presence or absence of catalysts, and reactor type) (Sharrudin et al., 2016).

During the recovery of polymers from WEEE, the greatest concern is the presence of halogenated flame retardants, which are often added to plastics to increase their resistance against ignition, slow combustion, and delay the spread of flames (Buekens and Yang., 2014). The most powerful fire suppressants available are brominated flame retardants, among which tetrabromobisphenol A (TBBA) is widely applied in various plastics used for electronics (Kousaiti, et al., 2020), including commercially available epoxy and PC resins (Levchik and Weil, 2006). In these resins, TBBA is generally used as a reactive flame retardant that is covalently bonded to the polymer matrix (Tolbäck et al., 2006).

Pyrolysis of TBBA-based polymers results in the generation of unwanted HBr and various bromo-organic products (Barontini et. al, 2004; Bozi et al., 2007), including harmful and toxic polybrominated dibenzo-p-dioxins and furans (PBDD/Fs) (Ortuño et al., 2014a). HBr emissions account for approximately 52% or more (up to 86%) of the initial bromine content of TBBA (Barontini et al., 2005) or TBBA epoxy resin (Grause et al., 2008). Bromine remaining in oil may account for up to 45% of the initial amount present in TBBA (Barontini et al., 2004). HBr gas is toxic and creates corrosive conditions in recycling facilities, while the presence of bromo-organic compounds in pyrolytic oil hinders its utilization.

Studies conducted in recent years have revealed that the use of some metal oxides (Terakado et al., 2011; 2013; Kumagai et al., 2017; Grabda et al., 2018) or metals (Oleszek

et al., 2013) in pyrolysis of TBBA-based polymers can lead to significant inhibition of brominated product emissions, due to free radical bromine fixation by the oxides or metals, followed by formation of stable metallic bromides or oxybromides.

For example, HBr emission from pyrolysis of printed circuit boards (PCBs) was reduced by approximately 80–90% in the presence of ZnO and La_2O_3 (1:2, w/w) (Terakado et al., 2013). Large amounts of added ZnO (PCB:ZnO, 1:20 w/w) also eliminated bromophenols from pyrolytic oil. A similar reduction in brominated products contained in gas and oil was reported with the use of La_2O_3 and CaO during pyrolysis with TBBA (Terakado et al., 2011). In the pyrolysis of phenols and epoxy-resin paper-laminated PCBs (Kumagai et al., 2017), brominated phenols and HBr emissions were reduced by 94% and 98%, respectively, in the presence of $Ca(OH)_2$. The main components of metallurgical dust (ZnO, PbO) showed positive effects on HBr emission from pyrolysis of PC based TBBA (PC-TBBA) (Grabda et al., 2018). In that study, however, pyrolytic products in oil were not quantified.

Copper is one of the main elements present in WEEE (Buekens and Yang, 2014; Hense et al., 2015). Depending on the WEEE composition (e.g. halogens content) and thermal conditions (e.g. inert or oxidative) the Cu can appear in various forms exhibiting different impact on degradation of the polymeric matrix and products distribution. There are several fundamental studies showing positive impact of Cu-based catalysts (e.g. Cu, CuO, and various Cu halides) on reducing emission of halogen containing compounds. However, none of these studies explain role of the Cu-based catalyst in debromination mechanism. Terakado et al., 2011 studied effect of CuO on pyrolysis of TBBA (1:2 w/w) about 50%, and over 90%, respectively. The CuO fixed the bromine in form of CuBr (400 ^{o}C) while the

unreacted CuO was reduced into metallic Cu (800 ^{o}C). Unfortunately, effect of the newly formed CuBr and Cu on the pyrolytic products generation was not considered in that study. Oleszek et al., 2013 tested metallic Cu on pyrolysis of TBBA-diglycidyl ether (1:5.16, w/w) at temperatures between 320 and 1000 °C with the aim of elucidating Cu translocation during pyrolysis of WEEE. About 50% of the Cu was transformed into CuBr (600 ^{o}C), while the unreacted Cu (50%) remained in metallic form. Unfortunately, the vaporized products in liquid fraction were not characterized and thus the effect of Cu on eventual debromination of the organic products remained unexplained. Grimes et. al, 2006 investigated individual copper compounds (Cu, CuO, and $CuCl_2$) on thermal behavior of polyvinyl chloride (PVC) at mass ratio of 1:9, w/w. It was reported that these compounds retarded degradation of the PVC and decreased volatile products at initial stage (300 ^{o}C) and advanced (600 ^{o}C) degradation stages. The Cu and CuO, both had positive impact on minimization of the HCl emission due to reaction of chlorine with the inorganic phase, as suggested by the authors, while such impact was not observed in presence of the $CuCl_2$ as this salt would not be able to take up any extra chlorine by chemical reaction, as it was stated by the authors. Emission of chloro-organic products was significantly reduced in both nitrogen and air atmosphere, with the greatest minimization for PVC-CuO and PVC-$CuCl_2$ mixtures. The CuO and $CuCl_2$ were found to also be more effective in reducing of aromatic products which was associated with much more effective polymer cross-linking than in the presence of metallic Cu. In regards to composition of the liquid fraction the most toxic representative of polychlorinated dibenzo-p-dioxin congeners, namely the 2,3,7,8-tetrachlorinated dibenzo-p- dioxin (TCDD), was detected in all mixtures treated

thermally in the air with an increased amount in the following order CuO<$CuCl_2$<Cu. In the inert atmosphere this congener was generated only in presence of CuO. Interestingly, for different CuO concentrations added to PVC (5, 10, and 20%) the quantities of the 2,3,7,8-TCDD together with other chlorinated and non-chlorinated products were comparable.

In contrast to the above-mentioned Cu compounds, there is no investigation concerning the impact of Cu_2O on the bromine flame retarded polymers degradation including its eventual influence on reduction of the brominated compounds emission. The available investigations are dedicated mainly to the Cu_2O impact on controlling flame retardance and smoke emission from PVC (Pike et al., 1997), polyurethane foam (Yuan et al., 2020) or epoxy resin (Chen et al., 2015).

Therefore, the present study aims to investigate the pyrolysis of PC-TBBA under non-catalytic and catalytic conditions using Cu_2O, with an emphasis on the distribution of bromine compounds within the solid, liquid, and gas fractions. The yields and compositions of each fraction were analyzed at three temperatures, corresponding to the initial, advanced, and complete pyrolytic degradation of PC-TBBA. The effects of Cu_2O and its products (CuBr and Cu) on PC-TBBA degradation at the tested temperatures were investigated thoroughly. To our knowledge this is the first study that explains stepwise impact of Cu_2O catalyst and the newly formed CuBr and Cu on pyrolysis of bromine flame retarded polymer.

2. Materials and Methods

2.1 Materials

177 The composition of the polymer material was provided by the supplier (Table 1). Its
178 elemental composition (H, O, C, and Br) was analyzed in this study using an organic
179 halogen/sulphur measurement system, YHS-11 (Yanaco, Co. Ltd.), with an analytical
180 accuracy of ±0.3%. Copper (I) oxide (Cu_2O) was purchased from Kanto Chemical Co. The
181 BET specific surface area of Cu_2O (Table 1) was determined using nitrogen adsorption at
182 −196 °C with an ASAP 2020 analyzer (Micromeritics, Norcross, GA, USA). The catalyst
183 was degassed at 25 °C before BET measurements. The total pore volume and average pore
184 diameter were determined using the Barrett, Joyner, and Halenda method. Sodium hydroxide
185 solution (NaOH, N/10), tetrahydrofuran (THF, 99.5%, dehydrated and stabilizer-free), and
186 anion-mixed standard solution were obtained from Kanto Chemical Co. The bromide (Br^-,
187 1000 mg/L) and copper (Cu 100 mg/L) ion standard solutions were obtained from Wako
188 Pure Chemical Co. (Japan). Naphthalene was supplied by Tokyo Chemical Industry. A
189 standard gas mixture (H_2, CO, CO_2, CH_4, and C_2-C_4 hydrocarbons) was purchased from
190 Tanuma Sasno Shoukai KK.
191
192 **2.2 Sample preparation**
193 Samples of commercial pelletized PC-TBBA resin were ground into coarse powder using
194 the Wonder Blender (Osaka Chemical, Co., Ltd.) and then milled in a planetary mill
195 (Pulverisette 6, Fritsch GmbH) at 300 rpm to obtain very fine powder. The powder
196 fractions were separated by sieving through a stainless-steel mesh sieve set (Nonaka-Rikaki
197 Co., Ltd.). The particle size was determined based on a laser diffraction and scattering
198 method using the Microtrac MT 3300EX. The particle size of PC-TBBA used in all

experiments was less than 53 μm. A mixture of the PC-TBBA with Cu_2O was manually mixed in a laboratory mortar, at mass ratio of 3.8:1 (w/w). This ratio was determined from their stoichiometric relationship, assuming all bromine present in PC-TBBA can be released and reacts with all copper present to form copper bromide.

2.3 Methods

2.3.1 Thermogravimetric analysis (TGA)

Thermal characterization of PC-TBBA and PC-TBBA+Cu_2O was performed using the Rigaku Thermo Plus TG 8120 analyzer. An individual sample of approximately 0.5 mg was placed into an open alumina pan and heated from 100 to 600 °C at a constant rate of 10 °C/min under helium flow of 100 mL/min. TGA was conducted three times for each sample to ensure repeatability and confirm the mixture homogeneity. Based on the TGA results, individual temperatures were selected corresponding to the initial (390 °C), advanced (480 °C), and complete (600 °C) degradation stages of pure PC-TBBA for application in further investigations using the horizontal fixed bed reactor.

2.3.2 Evolved gas analysis by mass spectrometry (EGA-MS)

Measurements were performed using a pyrolyzer coupled to a gas chromatography/mass spectrometry (GC/MS) system equipped with the Ultra ALLOY deactivated metal capillary tube UADTM (2.5 m, 0.15 mm i.d., Frontier Laboratories). An individual sample of approximately 0.5 mg was placed in a small Pt sample cup and heated from 50 to 600 °C at a heating rate of 10 °C/min under helium gas flow (100 mL/min). Prior to measurement, the

Pt sample cup was burned to remove all impurities. The GC/MS conditions were as follows: split injection mode, 100:1; column flow rate, 1 mL/min; oven and inlet temperature, 300 °C; mass scan range, 10–600.

Note: As the samples were pyrolyzed using the same temperature program as that used for TGA (10 °C/min), simultaneous detection of volatile products during the pyrolysis of PC-TBBA and PC-TBBA+Cu_2O was possible.

2.3.3 Fixed bed reactor

A horizontal quartz tube reactor (32 cm length, 0.7 cm i.d.) was heated using a ceramic electric tube furnace (ARF-20 KC). Schematic diagram of the experimental set-up is shown on Fig. 1. An individual sample (PC-TBBA; PC-TBBA+Cu_2O, 3.8:1, *w/w*) of approximately 0.2 g was placed in the center of the quartz tube reactor and held in place with glass quartz wool. The atmosphere inside the reactor was filled with helium at a flow rate of 50 mL/min for approximately 20–30 min prior to heating. The furnace was heated from ambient conditions to the desired temperature (390, 480 and 600 °C) at a heating rate of 10 °C/min. The vaporized components were transported to an aluminum bag (AAK-10, GL Science) via a nitrogen-cooled condenser and glass trap filled with NaOH solution. After the experiment, the tube reactor was cooled to ambient temperature, and then the condenser was defrosted under a continuous flow of helium to ensure the transfer of light gases into the aluminum bag. The products obtained from pyrolysis were defined as: *light gases* (collected in an aluminum bag), *HBr gas* (collected in an NaOH trap), *condensate* (collected in a condenser), and *residue* (remaining in a quartz tube reactor).

2.3.3.1 Quantification of pyrolytic products

Light gases were identified and quantified using gas chromatography coupled with a thermal conductivity detector (GC-TCD; GC323, GL Science) and a flame ionization detector (GC-FID; GC4000, GL Science) by comparison with standard gases.

HBr gas trapped in the NaOH solution was quantified via ion chromatography (Dionex ICS-1500) using an external standard curve.

Condensate was washed out of the condenser and quartz tube reactor wall with THF (~20 mL). The THF solution was divided into two portions. The first portion was mixed with naphthalene and used as an internal standard for the quantification of compounds using GC-FID. The second portion was applied to identification of the products using GC (7890A) combined with a mass spectrometer detector (MSD, 5975C) (Agilent Technologies).

Residue was characterized by X-ray diffraction (Rigaku, Rint 220) using Cu Kα1 radiation (1.54059 Å). Particle observations were conducted, and the elemental compositions of samples were analyzed using a scanning electron microscope with energy dispersive spectroscopy (SEM-EDS; JSM-5600T equipped with JED-23000U, JEOL). A sample weighing a few milligrams was mounted on a sample holder using carbon tape and then coated with Pt using a coater machine (JFC-1600, JEOL). Secondary electron images of the samples were obtained using an acceleration voltage of 15 keV for the electron beam. X-ray fluorescence emitted from the surface was collected and analyzed using the EDS system. Total X-ray emission measurements and spot analyses were conducted for 50–100 s. Mapping analyses were performed for 2.5 min per observation area. Functional groups in

the samples were analyzed using Fourier transform infrared spectroscopy (FT-IR; IR Affinity-1, Shimadzu Co.). A sample of 2 mg was mixed with 100 mg KBr in a mortar and pressed into a pellet using a hydraulic press (HAND PRESS SSP-10A, Shimadzu Co.). FT-IR spectra were collected within the range of 400 to 4000 cm^{-1} (resolution: 4 cm^{-1}, 128 scans) in transmission mode.

The total amount of Cu in all samples was determined by sample digestion with nitric acid (69%) using a microwave (ACTAC, Speedwave 4) and then quantified by inductively coupled plasma with atomic emission spectrometry (ICP-AES-SII Nanotechnology Inc., SPS-3500) using an external standard curve. Note: To confirm homogeneity of the raw mixture, the total amount of Cu was determined twice in randomly collected samples. Total bromine in the raw samples and residues was quantified by combustion ion chromatography (CIC), (AQF-2100H, Mitsubishi Chemical Analytech / HIC-20ASP, Shimadzu) following the procedure of Mukai et al., 2019. The bromine mass balance for each temperature was investigated using the measured quantities of bromine in residues before (Br_{solid}) and after ($Br_{residue}$) pyrolysis, as well as that in pyrolytic gas (Br_{gas}). The amount of bromine in condensate ($Br_{condensate}$) was estimated according to Eq. 1:

$$Br_{condensate} = Br_{solid} - (Br_{residue} + Br_{gas}) \quad (1)$$

Application of this calculation prevented potential underestimation of bromine due to the presence of non-identified bromo-organic compounds in the condensate fraction.

3. Results and Discussion

3.1 TGA results

The results from pyrolysis of PC-TBBA alone and in combination with Cu_2O (PC-TBBA+Cu_2O; 3.8:1 w/w) are presented in Fig. 2a. These results show that degradation of PC-TBBA alone generally proceeded in one step at temperatures between 380 °C and 550 °C and was accompanied by weight loss of approximately 68%. Further degradation up to 600 °C showed negligible loss weight of approximately 2%, with 30% remaining as residue. A slightly greater weight loss (76%) was reported for PC mixed with TBBA at 550 °C (Bozi et al., 2007), followed by negligible weight loss (~4%) during further heating to 900 °C, confirming that the main degradation step of PC-TBBA occurs below 600 °C

For the mixture of PC-TBBA+Cu_2O (Fig. 2a), degradation proceeded in one step between 450 and 550 °C, with a total weight loss of approximately 46%. Assuming that only the organic fraction vaporizes in this temperatures range, this weight loss corresponded to approximately 57% of the total vaporization products from pyrolysis of PC-TBBA. Notably, the presence of Cu_2O retarded vaporization by approximately 70 °C and significantly reduced the volume of the vaporized fraction by approximately 11% relative to pure PC-TBBA (Fig. 2a).

3.2 EGA-MS results

The total ion chromatogram (TIC) obtained from EGA-MS measurements (Fig. 2b) corresponded well with the derivative thermogravimetric (DTG) curves (Fig. 2a), but the TIC maxima were lower by approximately 5 and 3 °C relative to the DTG curves for PC-

309 TBBA and PC-TBBA+Cu_2O, respectively. Based on the mass spectra obtained at these TIC
310 maxima (data not shown), the dominant m/z ions were extracted (Fig. 3).
311 For pure PC-TBBA (Fig. 23), the first degradation step occurred within the range of 270–
312 350 °C and was initiated by the evolution of alkyl phenols (*m/z*=150), likely *p*-
313 isopropylphenol. The weight loss at these temperatures was 0.4% based on TGA (Fig. 2a).
314 The second degradation step began at approximately 370 °C with the evolution of CO_2
315 (*m/z*=44), phenol (*m/z*=94), diphenyl carbonate (*m/z*=214), and brominated compounds
316 (*m/z*=82, 172, and 252). The evolution of bisphenol A (*m/z*=228) began at approximately
317 390 °C. Vaporization of these products corresponded to the main degradation step observed
318 in the TGA (Fig. 2a). The third degradation stage was characterized by a shoulder at
319 approximately 440 °C in the profiles of phenol (*m/z*=94) and bromophenols (*m/z*=172 and
320 252), corresponding to the maxima at evolved *m/z*=214 and 228. The profiles obtained here
321 indicate that degradation of PC-TBBA follows various pathways (Fig. S1), with chain
322 scission of isopropylidene linkages (-C-$(CH_3)_2$-C-) and alcoholysis/hydrolysis of carbonate
323 linkages (-O-CO-O-) being the main degradation pathways (Jang and Wilkie, 2004; Blazsó
324 and Czégény, 2006). Early evolution of *p*-isopropylphenol indicates that chain scission
325 initiates the degradation of PC-TBBA. This result is in accordance with recent findings
326 (Siddiqui et al., 2018), in which *p*-isopropylphenol was detected as the first vaporization
327 product at the lowest temperature during pyrolysis of pure PC, and it also agrees with the
328 PC degradation pathways identified using the bond dissociation theory (Jang and Wilkie,
329 2004). The likely pathway of brominated products evolution (*m/z*=172 and 252) is chain
330 scission of the TBBA molecule (Fig. S1). The profile of HBr (*m/z*=82) evolution, with its

maximum at 413 °C, indicates that this product is not generated directly from TBBA (the lowest dissociation energy of the C-Br bond), but rather from bromophenols with maxima at 406 °C (*m/z*=252) and 411 °C (*m/z*=172) (Fig. 3). These bromophenols, via progressive debromination, were also a source of phenol (*m/z*=94) evolution during the third degradation step. The evolution of all products from PC-TBBA occurred below 600 °C.

Pyrolysis of PC-TBBA in the presence of Cu_2O: The TIC (Fig. 2b) was in good agreement with the DTG and TGA curves (Fig. 2a), confirming that the evolution of products is inhibited in the presence of Cu_2O. The extracted ions evolution profiles differed meaningfully from those of pure PC-TBBA (Fig. 3). The first degradation step (310–400 °C), associated with the evolution of alkyl phenols (*m/z*=150), corresponded to 1% vaporization of PC-TBBA (TGA, Fig. 2a). This initial weight loss was over two times greater than that of pure PC-TBBA, showing the catalytic impact of Cu_2O on PC-TBBA degradation. In the second degradation step (~400 °C), slow evolution of CO_2 and continuous evaporation of alkyl phenols (*m/z*=150) occurred simultaneously, while the evolution of other compounds shifted to approximately 460 °C. In contrast to the results from pure PC-TBBA, the extended evolution of CO_2 (400–460 °C) may be associated with enhanced char degradation due to the presence of Cu_2O, while at temperatures over 460 °C, enhanced decarboxylation may occur. On the other hand, lower intensities in the evolution profiles of other products indicate that in presence of Cu_2O vaporization of pyrolytic products is reduced, which may result from its influence on the cross-linking of the polymer, similarly as it was suggested in presence of CuO (Grimes et al., 2006). The evolution profiles of HBr and bromophenols are similar, with maxima at 506 °C (*m/z*=82

353 and 172) and 508 °C (*m/z*=252). However, the intensities of evolved ions of *m/z*=82 and
354 252 were significantly lower than those obtained during the non-catalytic run of pure PC-
355 TBBA, indicating that Cu_2O reduces the vaporization of brominated products. It might be
356 associated with the above-mentioned cross linking of the polymer as well as ability of the
357 Cu_2O to abstract the bromine forming CuBr. Evolution of di-bromophenols ceased at
358 approximately 530 °C, whereas that of HBr and mono-bromophenols continued, suggesting
359 further debromination. Vaporization of all products from PC-TBBA+Cu_2O was completed
360 by 550 °C (Fig. 3). Detailed investigations leading to explanation the reductive impact of
361 Cu_2O on brominated and non-brominated products from pyrolysis of PC-TBBA were
362 performed based on the results obtained from the fixed bed reactor.
363

364 **3.3 Fixed bed reactor results**

365 **3.3.1 Mass fraction distribution**

366 The total mass balance for all pyrolysis products of PC-TBBA and PC-TBBA+Cu_2O is
367 shown in Table S1. The high recovery rates (97% and 104%) confirmed that the reliability
368 of the results obtained here. The percentage distribution (calculated from the initial amount
369 of PC-TBBA in each sample) for all fractions (gas, condensate, and residue) and the
370 compositions of the individual vaporized fractions are shown in Table 2.
371 During pyrolysis of pure PC-TBBA at 390 °C, the gas, condensate, and residue fractions
372 accounted for 7.9, 14.8, and 76.4 wt.%, respectively (Table 2). With increased pyrolysis
373 temperatures of 480 and 600 °C, the condensates increased to 48.9 and 53.8 wt.%, while
374 the residue fractions decreased to 41.2 and 36.9 wt.%, respectively. The masses of the gas

fractions (12.5 and 11.6 wt.%) were comparable at these two temperatures. This finding indicates that the pyrolysis of pure PC-TBBA is nearly complete at 480 °C, and further heating to 600 °C does not meaningfully affect the mass distribution. The percentage distribution of the vaporized (condensate + gas) and residue fractions at 600 °C is in accordance with the mass loss and residue amounts obtained by TGA measurement (Fig. 2a).

An entirely different distribution was observed for pyrolysis of PC-TBBA in the presence of Cu_2O (Tables 2). At 390 °C, the gas (0.4 wt.%) and condensate (1.4 wt.%) fractions were approximately 16 and 10 times lower, respectively, compared with those from pyrolysis of pure PC-TBBA. At 480 °C, the gas and condensate fractions increased to 3.9 and 21%, respectively, leaving 71.2 wt.% residue. Further heating to 600 °C led to significant increases in the gas (8.4 wt.%) and condensate (44.6 wt.%) fractions. Residue (organic fraction only) accounted for 50.8 wt.% of the initial weight of PC-TBBA. These results indicate that Cu_2O reduces the yield of vaporization products by approximately 12% (600 °C), which agrees well with the results of TGA (Fig. 2a) and EGA-MS (Fig. 3).

3.3.1.1 Characterization of products in the gas fraction

During pyrolysis of pure PC-TBBA, HBr was the predominant product, accounting for 6.5, 7.4, and 7.5 wt.% of the initial PC-TBBA amount at 390, 480, and 600 °C, respectively (Table 2). At all temperatures, CO was significantly dominant over CO_2, reaching 18, 25, and 31% of the total gas fraction. No alkanes (CH_4 and C_2H_6) were detected at 390 °C, but trace amounts were measured at 480 and 600 °C.

Pyrolysis of PC-TBBA in the presence of Cu_2O markedly changed the chemical composition of the gas fraction (Table 2). The contribution of HBr was notably decreased, accounting for 0.3 wt.% at 390 and 480 °C and 1.2 wt.% at 600 °C. The level of CO_2, in contrast to pure PC-TBBA pyrolysis, was higher than that of CO at all temperatures, accounting for 25% (390 °C), 73% (480 °C), and 55% (600 °C) of the total gas fraction. At 600 °C, notable increases in the levels of CH_4 and C_2H_6 were observed. Traces of C_3H_8 were measured only at the highest pyrolysis temperature.

3.3.1.2 Characterization of organic products in the condensate

Among the products identified in the condensate, the most abundant were phenols, carbonyls, ethers, aromatics, and their brominated derivatives (Table 2).

For pyrolysis of PC-TBBA, non-brominated phenols represented the largest fraction, reaching a maximum of 24.3 wt.%, corresponding to 45% of the total condensate produced at 600 °C. At all temperatures, single-ring phenolic compounds were more abundant than those with two rings. At 390 °C, phenol and alkyl phenols were most abundant, whereas at 480 and 600 °C, phenol and 4,4`-(1-methylethylidene)bisphenol were most abundant. Diphenyl carbonate, which is the main component of PC polymer, was the most abundant of the carbonyls produced at all temperatures evaluated. The detected bromo-organic products matched those identified from the degradation of PC-TBBA by Bozi et al., 2007 and by Blazsó and Czégény, 2006. Most bromo-organic products are brominated derivatives of phenol (Table 2), with dominance of 2,4-dibromophenol over 2,3,5-tribromophenol, and mono-bromophenols. The products in *ortho*- and *para*- bromine

substitution (e.g. 2-bromophenol and 2,4-dibromophenol) are known to be the most likely precursors of PBDD/Fs generated via thermal processes of polymers containing TBBA (Barontini and Cozzani, 2006, Ortuño et al., 2014b; Luijik and Govers, 1992). In this study, however, PBDD/Fs were not detected at any pyrolysis temperature, although the presence of a small amount (below 0.05 wt.%) of non-bromine substituted dibenzofuran was detected within all studied temperatures. The results are consistent with that of Barontini and Cozzani, 2006 who evidently showed, that the PBDD/Fs are most likely formed in oxidative rather than pyrolytic treatment of various cross-linked epoxy resins containing TBBA. On the other hand, various PBDD/Fs yielding predominantly tetra-brominated congeners (Ortuño et al., 2014b) and mono- through penta-brominated congeners (Luijik and Govers, 1992), have been detected in pyrolysis of TBBA and ABS/TBBA blend, respectively. The measured quantities, however, were at a level of ppb. Considering that the detection limit of applied procedure in this study is at level of ppm, eventual presence of the lower brominated congeners of PBDD/Fs in the liquid fraction cannot be excluded. Organo-bromine compounds accounted for 1, 2, and 3 wt.% of the initial amount of PC-TBBA at 390, 480, and 600 °C, respectively (Table 2).

The presence of Cu_2O significantly altered the distribution of products present in the condensate (Table 2). At 390 °C, few compounds were detected at trace levels; surprisingly, no phenol was detected, despite constituting 3.1 wt.% of the pyrolysis products from pure PC-TBBA.

At a higher pyrolysis temperature (480 °C), the vaporization of liquid products increased, but the quantities of phenol and its derivatives were significantly lower relative to their

441 evolution from pure PC-TBBA. The same pattern was observed for all brominated phenols
442 except tribromophenol. Significant differences in the product distribution between non-
443 catalytic and catalytic runs were observed at 600 °C. Among phenols, alkyl phenols such as
444 4-methyl phenol and 4-ethyl phenol were dominant, with quantities higher than those from
445 pure PC-TBBA (600 °C). Increased amounts of vaporized ethers were observed, in contrast
446 to the non-catalytic run. Among the brominated products, 3-bromo-1-propanol was
447 dominant, reaching 0.4 wt.% (Table 2). All other brominated products were detected at
448 quantities below 0.1 wt.% at 600 °C. In contrast to the non-catalytic run, the brominated
449 phenols have not been detected at 390 °C, while in the higher temperatures their quantities
450 were significantly lower. At 600 °C, the mono-bromophenols quantities dominated over
451 2,4-dibromophenol indicating its gradual debromination, which simultaneously resulted in
452 increased amounts of HBr. This results well agree with the EGA-MS observations (Fig. 3).
453 A similarly significant reduction in brominated phenols emission was noted in pyrolysis of
454 TBBA with CuO (Terakado et al., 2011). However, the reduction in brominated phenols
455 was simultaneous with generation of phenol which amount was considerably higher than
456 from pyrolysis of pure TBBA. The mechanism was not explained but authors suggested
457 that the CuO enhances bromine abstraction from organic molecule generating CuBr.
458 Results collected in Table 2 shows, that in presence of Cu_2O the debromination may occur
459 to some extent due to bromine fixation in form of salt, but there is evident decrease in
460 evolution of all products what might be associated with effective cross-linking of the
461 organic products in the Cu_2O presence, as suggested by Grimes et al., 2006. The PBDD/Fs,
462 similarly to the non-catalytic runs, have not been detected at any of the studied

463 temperatures. Comparative study (Ortuño et al., 2014b) on PBDD/Fs from pyrolysis (600
464 ^{o}C) of waste PCBs with and without metallic fraction (dominated by presence of Cu)
465 revealed quantities at level of ppb with tendency in reducing of these compounds in the
466 presence of metallic fractions.
467 The total level of organo-bromine products was reduced significantly in the presence of
468 Cu_2O, accounting for 0.2 wt.% (480 °C) or 0.9 wt.% (600 °C) of the initial amount of PC-
469 TBBA, which corresponded to 1–2% of the total condensate (Table 2). For comparison,
470 total brominated compounds detected from pyrolysis of pure PC-TBBA at the same
471 temperatures accounted for 6–7% of the total condensate fraction.
472
473 **3.3.1.3 Composition of the residues**
474 Characterization of the raw (unheated) samples and residues from pyrolysis of PC-TBBA
475 and PC-TBBA+Cu_2O at various temperatures was performed using FT-IR (Fig. 4, Table 3).
476 The IR spectra of the raw samples were compared with that of reference PC (Fig. 4a). The
477 most significant peaks were assigned according to Silverstein et al., 1991 (Table 3) and
478 compared with previously reported data for PC (Politou, et al., 1990; Jang and Wilkie,
479 2005).
480 The IR spectrum of raw PC-TBBA was comparable with that of reference PC (Fig. 4a),
481 indicating that PC is the main component of the polymer. The most intense peak at 1770
482 cm^{-1} corresponded to the carbonate functional group. The contributions of aromatic
483 structures were indicated by peaks at 1504, 1408, and 1080 cm^{-1}. The peaks at 1504 and
484 828 cm^{-1} were characteristic of para-substituted aromatic rings, while that at 1080 cm^{-1}

485 represented the aryloxy group in aromatic rings. The peak at 2968 cm^{-1} was attributed to the
486 methyl group.
487 The IR spectrum (Fig. 4a) of the residue obtained from pyrolysis of PC-TBBA at 390 °C
488 was very similar to that of the raw sample, but an increase in intensity was evident. This
489 intact structure of the polymer indicated its high thermal stability even if the total amount
490 of generated gases was about 24 wt. % in this temperature (Table 2). A new broad peak
491 appeared at approximately 3500 cm^{-1}, associated with formation of the phenolic (-OH)
492 group. These results are compatible with those of Politou et al., 1990, who reported that PC
493 resin remains essentially intact up to 400 °C. The spectrum at 480 °C was significantly
494 different. The C-H stretch region (approximately 3000 cm^{-1}) nearly disappeared, while the
495 aromatic band (at ~3040 cm^{-1}) grew. The carbonate group (1770 cm^{-1}), which was almost
496 eliminated from the residue, was eclipsed by the growing C=O stretch of aromatic esters
497 (~1742 cm^{-1}). The aromatic bands (1080, and 1408 cm^{-1}) and CH_3 deformation band (1364
498 cm^{-1}) were no longer detectable. At 600 °C, almost all functional groups were eliminated,
499 and the remaining bands at 1606 and 3040 cm^{-1} indicated that some aromatics remained in
500 the residue (Politou et al., 1990). These results indicate that above 390 °C, extensive
501 thermal branching and crosslinking occur, and as a result, esters or unsaturated hydrocarbon
502 bridges are formed (Politou et al., 1990).
503 The IR spectrum of raw PC-TBBA+Cu_2O (Fig. 4b) was similar to that of raw PC-TBBA,
504 with the exception of an intense peak at 630 cm^{-1}, which may be assigned to the Cu-O bond
505 (Silverstein et al., 1991). At 390 °C, all functional groups were present in the residue, with
506 no change in the positions of the peaks, but lower intensities of all peaks relative to pure

PC-TBBA. In this temperature mass loss of the polymer was of about 1% (Table 2). The residue collected at 390 ºC was in form of melted solid of high viscosity and the color of the residue was like the initial color of raw mixture (dark red). It suggested that the Cu_2O particles diffuse within the melted polymer matrix resulting in interactions between organic layer and inorganic particles lowering relative intensities of functional group peaks. At 480 °C (Fig. S2, Supplementary material), most functional groups remained present in the residue, including the phenolic group. In contrast to pure PC-TBBA, the intensities of bands attributed to aromatics (1080, 1504, 1606 cm^{-1}) and the carbonate group (1773 cm^{-1}) were stronger. Decreased intensity of the Cu-O band can be observed. The IR spectrum of the residue formed at 600 °C indicates complete degradation of the polymer (Fig. 4b). X-ray diffraction of the residues (Fig. 5) obtained at increasing temperatures showed that Cu_2O (390 °C) undergoes bromination to CuBr followed by progressive reduction to Cu, which was the dominant pattern at 480 and 600 °C, respectively. The level of Cu was stable during pyrolysis (Table S1), and Cu remained in the residue at all tested temperatures. In contrast to the raw sample of PC-TBBA+Cu_2O, SEM morphological analysis of the pyrolytic residues (Fig. 6) showed compacted layers at all temperatures, in which C, O, and Br were uniformly dispersed. Cu-O, Cu-Br, and Cu particles were distributed across the degraded polymer surfaces at 390, 480, and 600 °C, respectively.

As Cu_2O undergoes successive changes at increasing pyrolysis temperatures, not only Cu_2O but also newly formed copper compounds must affect polymer degradation and the product distribution at each temperature.

3.3.2 Suggested impacts of Cu_2O on mitigation of brominated compounds emission and the newly formed copper compounds (CuBr, and Cu) on further degradation of the polymer at specific pyrolysis temperatures.

(a) At the initial stage of PC-TBBA pyrolysis (up to 390 °C), Cu_2O mediated early cross-linking of polymers through cross-coupling "Ullman" reactions (Fig. 7). Ullman was the first to report that at temperatures above 200 °C, copper mediates C-C coupling via radical or nucleophilic oxidative addition followed by reductive elimination (Mondal, 2016; Beletskaya and Cheprakov, 2004; Li and Lan, 2020). As illustrated in the schematic diagrams (Fig. 7a–c), these reactions also generate CuBr. The reductive coupling mechanism was shown in pyrolysis of PVC in presence of transition metal (MnO_3) which involved oxidation of a low-valency state of the transition metal generated under pyrolytic conditions by reaction with a chlorine atom of the polymer chain to form a metal chloride and a cross-link polymer (Lattimer and Kroenke 1993). Similar reductive coupling mechanism was reported in presence of various Cu halides (CuBr, CuCl, and CuI) on PVC pyrolysis (Müller and Dongman, 1998). It seems that the proposed mechanism (Fig. 7) is the mostly responsible for effective mitigation in vaporization of the bromo-organic products. However, the reaction of Cu_2O (Eq. 2) with HBr cannot be excluded as it is thermodynamically favored at this temperature ($\Delta G^0_r = -70$ kJ/mol) (Shibata et al., 2006). This reaction could be the mostly responsible for mitigation in HBr vaporization.

$$Cu_2O_{(s,l)} + HBr_{(g)} \rightarrow CuBr_{(s)} + H_2O_{(g)} \quad (2)$$

551 It is important to mention, that the residue collected at 390 ^{o}C was in melted form of high
552 viscosity, of dark-red color as same as before pyrolysis. There was not visual indication on
553 carbonization of the residue in this temperature, what could be a confirmation, that the
554 cross-linking through the "Ullman" reactions is the main mechanism responsible for
555 effective reduction in bromo-organic products vaporization.
556 (b) At 390–480 °C, cross-linking of the polymer continued, and char formation
557 occurred (the color of residue collected at 480 ^{o}C was a dark brown). It was already
558 reported (Pike et al., 1997, Lattimer and Kroenke, 1981) that the cross-linking of polymer
559 (e.g. PVC) in presence of Cu compounds increases amount of char while decreases number
560 of volatile products and reduce formation of aromatic products. It is associated with
561 reduction in the heat and mass transfers in charring polymer which influence the thermal
562 degradation of polymer matrix (Pike et al., 1997). The CO was formed by char
563 decomposition; however, in the presence of Cu_2O, this gas was efficiently utilized to
564 generate CO_2 (Eq. 3a and b). This positive effect of Cu_2O on efficient conversion of CO to
565 CO_2 was previously reported by Chen et al., 2015, who observed it during pyrolysis of
566 epoxy resin, while CO suppression by Cu(I) salts during pyrolysis of PVC was reported by
567 Pike et al., 1997.
568
569 $$Cu_2O_{(s,l)} + C_{(s)} \rightarrow 2Cu_{(s)} + CO_{(g)} \quad (3a)$$
570 $$Cu_2O_{(s,l)} + CO_{(g)} \rightarrow 2Cu_{(s)} + CO_{2(g)} \quad (3b)$$
571

572 (c) Over 480 °C, the residue contained Cu and CuBr. These two forms of copper are in
573 different oxidative states (Cu^{+} and Cu^{0}, respectively) and may have different impacts on
574 polymer degradation. However, it is impossible to discuss the effects of these copper
575 compounds separately. Based on the results of the present study (Table 2, Fig. 3), the
576 following suggestions can be drawn:
577 - Cu and CuBr promote decarboxylation. In contrast to pure PC-TBBA, an evident
578 decrease in vaporized carbonates occurs, with a simultaneous increase in ethers (Table 2,
579 600 °C). Antonakou et al., 2014 reported a similar catalytic effect with the pyrolysis of pure
580 PC in the presence of zeolites and basic metal oxides.
581 - Cu and CuBr promote degradation of bisphenol A, as its quantities are evidently
582 lower relative to the non-catalytic run of PC-TBBA pyrolysis (480 and 600 °C). Reduced
583 emission of bisphenol A during pyrolysis of PC with $CuCl_2$ was also reported by Šala et al.,
584 2010.
585 - Cu and CuBr evidently favor generation of 4-methyl and 4-ethyl phenols, which are
586 abundant in the condensate (600 °C, Table 2), in contrast to that of pure PC-TBBA. Similar
587 observations were reported during the pyrolysis (600 °C) of non-halogenated PC in the
588 presence of $CuCl_2$, (Blazsó, 1999), as well as zeolites, and basic metal oxides (Antonakou
589 et al., 2014).
590 - Debromination of bromo-organics is catalyzed in the presence of Cu, as HBr gas
591 emission increases at 600 °C. Cu has been suggested to catalyze the cleavage of the C-H
592 bond, causing hydrogen to be abstracted by the bromine radical (cleavage of the C-Br
593 bond), thus generating HBr. As the residue is degraded completely at 600 °C (Fig. 4b), this

debromination must occur at just over 480 °C. Debromination may lead to increased phenol production, which is evidently higher at 600 °C than at 480 °C (Table 2). This suggestion is supported by the EGA-MS results showing simultaneous evolution of HBr and bromophenols (Fig. 3).

- Significant charring of the residue occurs in the presence of copper compounds (Table 2). The char forms a protective layer, hindering vaporization of gases and liquids at the higher temperatures.

3.3.3 Bromine distribution within fractions

Total bromine quantities obtained from catalytic and non-catalytic pyrolysis of PC-TBBA are shown in Table 4. For pure PC-TBBA, the majority of bromine (51–59% of the total Br amount) was vaporized in the form of HBr gas (Table 2) at all temperatures tested. At the initial degradation temperature (390 °C), approximately 38% of Br was present in the residue, while 11% was in the condensate. Increasing the pyrolysis temperature to 480 and 600 °C caused a significant increase in Br-containing compounds in the condensate (~40%), while the remaining residues were almost free of bromine (2 and 0.5%).

Significant changes in the bromine distribution were observed in the presence of Cu_2O. The majority of the bromine remained in the residues. With increasing pyrolysis temperatures, the amount of remaining bromine decreased from 99% to 93% to 86%. In contrast to pure PC-TBBA, only trace amounts of bromine (2–3%) were present in the gas fractions produced at 390 and 480 °C, and the maximum amount (11%) was observed at 600 °C. The amounts of bromine in the condensate were 0.2% at 390 °C and 3–4% at 480 and 600 °C.

The condensate fraction yield at 600 °C was double that at 480 °C, and the Br amount was stable, which is encouraging from the perspective of further utilization of this product. In summary, the Br levels observed in the presence of Cu_2O (at the complete degradation temperature of 600 °C) were approximately 6 and 13 times lower in the gas and condensate fractions, respectively, relative to the corresponding levels obtained from non-catalytic pyrolysis of PC-TBBA.

4. Conclusions

Here, the products of pyrolysis of pure PC-TBBA and PC-TBBA in the presence of Cu_2O were investigated, with an emphasis on the generation and distribution of brominated compounds. Generally, the presence of Cu_2O reduced the quantities of gas and condensate produced in favor of residues. At the temperature of complete polymer degradation (600 °C), the condensate and gas fractions were approximately 9% and 4% lower than those generated from pyrolysis of pure PC-TBBA (54% and 12%, respectively). For both pure PC-TBBA and PC-TBBA+Cu_2O, the condensate was rich in valuable chemicals (phenols, carbonyls, ethers, and aromatics) but also contained some undesirable bromo-organic compounds originating from TBBA decomposition. However, Cu_2O significantly reduced these bromo-organic products in the condensate, which is important for further product recovery. Moreover, evolution of toxic HBr gas was meaningfully reduced in the presence of Cu_2O, accounting for only 1% of the initial amount of PC-TBBA at 600 °C.

Significant reduction of HBr evolution results from effective bromine fixation by oxides and formation of stable CuBr, which does not vaporize at temperatures up to 600 °C.

638 Meanwhile, a substantial decrease in organo-bromine products in the condensate was
639 associated with their involvement in coupling reactions that cause intermolecular cross-
640 linking by the copper compounds.
641 The results of this study indicate that Cu_2O is a strong transition metal oxide that can
642 readily shift to the oxidative state, thereby significantly impacting the degradation of
643 bromine-containing polymers. Therefore, elucidating the roles of various copper
644 compounds in pyrolysis is essential to designing a process that effectively inhibits
645 vaporization of bromine compounds and enhances the generation of valuable gas and liquid
646 products.
647

648 **Appendix A: Supplementary Materials**

649 **Table S1.** Mass balance for pyrolysis experiments.
650 **Fig. S1.** Simplified initial pathways degradation based on thermal profiles from EGA-MS.
651 **Fig. S2.** Comparison of IR spectra of residues from pyrolysis of PC-TBBA, and PC-
652 TBBA+Cu_2O at 480 ºC.
653

654 **Acknowledgments**

655 This study was supported by a research grant from the Yonemori Seishin Ikuseikai
656 Foundation, Kagoshima, Japan. We would like to express our gratitude to the Advanced
657 Environmental System of the Department of Environmental Engineering at Kyoto
658 University for providing the SEM-EDS equipment. We would also like to express our
659 thanks to Prof. Itoh, Dr. Echigo, and Dr. Nakanishi of Kyoto University for providing the

660 FT-IR equipment and to Prof. Shibata of Tohoku University for providing the IC and ICP-
661 AES equipment.

662

663 **References**

664 GDFEEW, 2019. Decent work in the management of electrical and electronic waste (e-
665 waste), Issues paper for the Global Dialogue Forum on Decent Work in the Management of
666 Electrical and Electronic Waste (E-waste), Geneva, 9-11 April, 2019, International Labour
667 Office, Sectoral Policies Department, Geneva, ILO, 2019. ISBN 978-92-2-133079-0 (Web
668 pdf).

669 Kousaiti, A., Hahladakis, J.N., Savvilotidou, V., Pivnenko, K., Tyrovola, K.,
670 Xekoukoulotakis, N., Astrup, T.F., Gidarakos, E., 2020. Assessment of
671 tetrabromobisphenol-A (TBBPA) content in plastic waste recovered from WEEE. J. Hazard.
672 Mater. 390, 121641. https://doi.org/10.1016/j.jhazmat.2019.121641.

673 Levchik, S.V., Weil E.D., 2005. Overview on recent developments in the flame retardancy
674 of polycarbonates. Polym. Int. 54, 981-998. https://doi.org/10.1002/pi.1806.

675 Grigorescu, R.M., Grigore, M.E., Iancu, L., Ghioca, P., Ion, R.M., 2019. Waste electrical
676 and electronic equipment: A review on the identification methods for polymeric materials.
677 Recycling. 4, 32, 1-21. https://doi.org/10.3390/recycling4030032.

678 Chandrasekaran, S. R., Avasarala, S., Murali, D., Rajagopalan, N., Sharma, B. K., 2018.
679 Materials and energy recovery from E-waste plastics. ACS Sustainable Chem. Eng. 6, 4,
680 4594-4602. https://doi.org/10.1021/acssuschemeng.7b03282.

681 Sharrudin, S. D. A., Abnisa, F., Daud, W.M.A.W., Aroua, M. K.. 2016. A review on
682 pyrolysis of plastic waste. Energ. Convers. Manage. 115, 308-326.
683 https://doi.org/10.1016/j.enconman.2016.02.037.
684 Shen, J., Zhao, R., Wang, J., Chen, X., Ge, X., Chen, M., 2016. Waste-to-energy:
685 Dehalogenation of plastic-containing wastes. Waste Manage. 49, 287-303.
686 https://doi.org/10.1016/j.wasman.2015.12.024.
687 Buekens, A., Yang, J., 2014. Recycling of WEEE plastics: a review. J. Mater. Cycles Waste
688 Manag. 16, 415-434. https://doi.org/10.1007/s10163-014-0241-2.
689 Levchik, S.V., Weil, E.D., 2006. Flame retardants in commercial use or in advanced
690 development in polycarbonates and polycarbonate blends. J. Fire Sci. 24, 137-151.
691 https://doi.org/10.1177/0734904106055997.
692 Tollbäck, J., Crescenzi, C., Dyremark, E., 2006. Determination of the flame retardant
693 tetrabromobisphenol A in air samples by liquid chromatography- mass spectrometry. J.
694 Chromatogr. A. 1104, 106-112. https://doi.org/10.1016/j.chroma.2005.11.067.
695 Barontini, F., Cozzani, V., Marsanich, K., Raffa, V., Petarca L., 2004. An experimental
696 investigation of tetrabromobisphenol A decomposition pathways. J. Anal. Appl. Pyrol. 72,
697 41-53. https://doi.org/10.1016/j.jaap.2004.02.003.
698 Bozi, J., Czégény, Z., Mészáros E., Blazsó, M., 2007. Thermal decomposition of flame
699 retarded polycarbonates. J. Anal. Appl. Pyrol. 79, 337-345.
700 https://doi.org/10.1016/j.jaap.2007.01.001.

701 Ortuño, N., Moltó, J., Conesa, J.A., Font, R., 2014a. Formation of brominated pollutants
702 during the pyrolysis and combustion of tetrabromobisphenol A at different temperatures.
703 Environ. Pollut. 191, 31-37. https://doi.org/10.1016/j.envpol.2014.04.006
704 Barontini, F., Marsanich, K., Petarca, L., Cozzani, V., 2005. The thermal degradation
705 process of tetrabromobisphenol A. Ind. Eng. Chem. Res. 43, 1952-1961.
706 https://doi.org/10.1021/ie034017c.
707 Grause, G., Furusawa, M., Okuwaki, A., Yoshioka, T. 2008. Pyrolysis of
708 tetrabromobisphenol-A containing paper laminated printed circuit board. Chemosphere. 71,
709 872-878. https://doi.org/10.1016/j.chemosphere.2007.11.033.
710 Terakado, O., Ohhashi, R., Hirasawa, M., 2011. Thermal degradation study of
711 tetrabromobisphenol A under the presence metal oxide: comparison of bromine fixation
712 ability. J. Anal. Appl. Pyrol. 91, 303-309. https://doi.org/10.1016/j.jaap.2011.03.006.
713 Terakado, O., Ohhashi, R., Hirasawa, M. 2013. Bromine fixation by metal oxide in
714 pyrolysis of printed circuit board containing brominated flame retardants. J. Anal. Appl.
715 Pyrol. 103, 216-221. https://doi.org/10.1016/j.jaap.2012.10.022.
716 Kumagai, S., Grause, G., Kameda, T., Yoshioka, T., 2017. Thermal decomposition of
717 tetrabromobishphenol-A containing printed circuit boards in the presence of calcium
718 hydroxide. J. Mater. Cycles Waste Manag. 19, 282-293. https://doi.org/10.1007/s10163-
719 015-0417-4.
720 Grabda, M., Oleszek, S., Shibata, E., Nakamura, T. 2018. Distribution of inorganic bromine
721 and metals during co-combustion of polycarbonate (BrPC) and high-impact polystyrene

(BrHIPS) wastes containing brominated flame retardants (BFRs) with metallurgical dust. J. Mater. Cycles Waste Manag. 20, 201-213. https://doi.org/10.1007/s10163-016-0565-1.

Oleszek, S., Grabda, M., Shibata, E., Nakamura, T. 2013.Distribution of copper, silver, and gold during thermal treatment with brominated flame retardants. Waste Manage. 33, 1835-1842. https://doi.org/10.1016/j.wasman.2013.05.009.

Hense, P., Reh, K., Franke, M., Aigner, J., Hornung, A., Contin A., 2015. Pyrolysis of waste electrical and electronic equipment (WEEE) for recovering metals and energy: Previous achievements and current approaches. Environ. Eng. Manag. J. 7, 1637-1647. http://omicron.ch.tuiasi.ro/EEMJ/.

Grimes, S.M, Lateef, H., Jafari, A.J., Mehta, L., 2006. Studies of the effects of copper, copper(II) oxide and copper(II) chloride on thermal degradation of poly(vinyl chloride). Polym. Degrad. Stabil. 91, 3724-3280. https://doi.org/10.1016/j.polymdegradstab.2006.06.010.

Pike, R.D, Starnes, W.H., Jeng, J.P., Bryant, W.S., Kourtesis, P., Adams, Ch.W., Bunge, S.D., Kang, Y.M., Kim, A.S., Kim, J.H., Macko, J.A., O'Brien, Ch.P., 1997. Low valent metals as reductive cross-linking agents: A new strategy for smoke suppression of poly(vinyl chloride), Macromolecules. 30, 6957-6965. https://doi.org/10.1021/ma9707749.

Yuan Y., Wang W., Shi Y., Song L., Ma Ch., Hu Y. 2020. The influence of highly dispersed Cu_2O-anchored MoS_2 hybrids on reducing smoke toxicity and fire hazards for rigid polyurethane foam. J. Hazard. Materials, 382, 121028. https://doi.org/10.1016/j.jhazmat.2019.121028.

743 Chen, M.J., Lin, Y.Ch., Wang, X.N., Liu, Z., Li, Q.L., Liu, Z.G., 2015. Influence of
744 cuprous oxide on enhancing the flame retardancy and smoke suppression of epoxy resins
745 containing microencapsulated ammonium polyphosphate. Ind. Eng. Chem. Res. 54, 12705-
746 12713. https://doi.org/10.1021/acs.iecr.5b03877.
747 Mukai, K., Fujimori, T., Shiota K., Takaoka, M., Funakawa, S., Takeda A., Takahashi, S.,
748 2019. Quantitative speciation of insoluble chlorine in environmental solid samples. ACS
749 Omega. 4, 6126-6137. https://doi.org/10.1021/acsomega.9b00049.
750 Jang, B.N., Wilkie, C.A., 2004. A TGA/FTIR and mass spectral study on the thermal
751 degradation of bisphenol A polycarbonate. Polym. Degrad. Stab. 86, 419-430.
752 https://doi.org/10.1016/j.polymdegradstab.2004.05.009
753 Blazsó, M., Czégény, Z., 2006. Catalytic destruction of brominated aromatic compounds
754 studied in a catalyst microbed coupled to gas chromatography/mass spectrometry. J.
755 Chromatogr. A 1130, 91-96. https://doi.org/10.1016/j.chroma.2006.05.009.
756 Siddiqui, M.N., Redhwi, H.H., Antonakou, E.V., Achilias, D.S. 2018, Pyrolysis mechanism
757 and thermal degradation kinetics of poly(bisphenol A carbonate)-based polymers
758 originating in waste electric and electronic equipment. J. Anal. Appl. Pyrol. 132, 123-133.
759 https://doi.org/10.1016/j.jaap.2018.03.008.
760 Barontini, F., Cozanni, V., 2006. Formation of hydrogen bromide and organobrominated
761 compounds in the thermal degradation of electronic boards, J. Anal. Appl. Pyrol. 77, 41-55.
762 https://doi.org/10.1016/j.jaap.2006.01.003.

763 Ortuño N., Conesa J.A., Moltó J., Font R., 2014b. Pollutant emissions during pyrolysis and
764 combustion of waste printed circuit boards, before and after metal removal. J. Sci. Tot.
765 Environ. 449, 27-35. https://doi.org/10.1016/j.scitotenv.2014.08.039
766 Luijk R., Govers H.A.J., 1992. The formation of polybrominated dibenzo-p-dioxins
767 (PBDDs) and dibenzofurans (PBDFs) during pyrolysis of polymer blends containing
768 brominated flame retardants. Chemosphere 25, 361-374. https://doi.org/10.1016/0045-
769 6535(92)90553-4.
770 Silverstein, R.M., Bassler, G.C., Morrill, T.C., 1991. Spectrometric identification of
771 organic compounds, 5th Edition, John Wiley and Sons, Inc.
772 Politou, S., Morterra, C., Low, M.J.D., 1990. Infrared studies of carbons. XII The
773 formation of chars from a polycarbonate. Carbon 28, 529-538.
774 https://doi.org/10.1016/0008-6223(90)90049-5.
775 Jang, B.N., Wilkie, C.A., 2005. The thermal degradation of bisphenol A polycarbonate in
776 air, Thermochim. Acta. 426, 73-84. https://doi.org/10.1016/j.tca.2004.07.023.
777 Mondal, S., 2016. Recent advancement of Ullmann-type coupling reactions in the
778 formation of C–C bond. ChemTexts, 2, 17. https://doi.org/10.1007/s40828-016-0036-2.
779 Beletskaya, I.P., Cheprakov, A.V., 2004. Copper in cross-coupling reactions. The post
780 Ullman chemistry. Coordin. Chem. Rev. 248, 2337-2364.
781 https://doi.org/10.1016/j.ccr.2004.09.014.
782 Li, S.J., Lan, Y., 2020. Is Cu(III) a necessary intermediate in Cu-mediated coupling
783 reactions? A mechanistic point of view. Chem. Commun. 56, 6609-6619.
784 https://doi.org/10.1039/D0CC01946A.

785 Lattimer R.P., Kroenke W.J. 1981. The Functional Role of Molybdenum Trioxide as a
786 Smoke Retarder Additive in Rigid Poly(vinyl Chloride). J. Appl. Polym. Sci. 26, 1191-
787 1210.
788 Müller J., Dongman G. 1998. Formation of aromatics during pyrolysis of PVC in the
789 presence of metal chlorides. J. Anal. Appl. Pyrolysis, 45, 59-74.
790 Shibata, E., Grabda, M., Nakamura, T. 2006. Thermodynamic consideration of the
791 bromination reactions of inorganic compounds. J. Jpn. Soc. Waste Manage. Experts. 17,
792 361-371. (in Japanese).
793 Antonakou, E.V., Kalogiannis, K.G., Stefanidis, S.D., Karakoulia, S.A., Triantafyllidis,
794 K.S., Lappas, A.A., Achilias, D.S., 2014. Catalytic and thermal pyrolysis of polycarbonate
795 in a fixed-bed reactor: The effect of catalyst on products yields and composition. Polym.
796 Degrad. Stabil. 110, 482-491. http://dx.doi.org/10.1016/j.olymerdegradstab.2014.10.007.
797 Šala, M., Kitahara, Y., Takahashi, S., Fuji T., 2010. Effect of atmosphere and catalyst on
798 reducing bisphenol A (BPA) emission during thermal degradation of polycarbonate.
799 Chemosphere 78, 42-45. https://doi.org/10.1016/j.chemosphere.2009.10.036
800 Blazsó, M., 1999. Thermal decomposition of polymers modified by catalytic effects of
801 copper and iron chlorides. J. Anal. Appl. Pyrol. 51, 73–88. https://doi.org/10.1016/S0165-
802 2370(99)00009-1.
803
804 **List of Captions:**
805 **Fig. 1.** Schematic diagram of the experimental set-up and overview of the analytical
806 methods: (1) helium cylinder, (2) flow meter, (3) electric furnace, (4) thermocouple, (5)

807 quartz tube reactor, (6) glass quartz wool, (7) sample/residue location, (8) liquid nitrogen-
808 cooled condenser, (9) HBr trap in NaOH solution, (10) aluminum gas bag.
809 **Fig. 2.** TG and DTG curves (a), and TIC (b) for PC-TBBA and PC-TBBA+Cu_2O (3.8:1
810 *w/w*) under He flow.
811 **Fig. 3.** Temperature dependent TIC and extracted ion chromatograms obtained from EGA-
812 MS.
813 **Fig. 4.** Comparison of IR spectra of raw samples and residues from pyrolysis of PC-TBBA
814 (A), and PC-TBBA+Cu_2O (B).
815 **Fig. 5.** XRD results of residues at various temperatures of pyrolysis of PC-TBBA+Cu_2O.
816 **Fig. 6.** SEM results of residues obtained at various temperatures of pyrolysis of PC-
817 TBBA+Cu_2O.
818 **Fig. 7.** Schemes of copper mediated coupling reactions generating cross-linking of polymer
819 and CuBr.
820 **Table 1.** Composition of polycarbonate based tetrabromobisphenol A (PC-TBBA) and
821 catalyst (Cu_2O) BET surface area characteristic.
822 **Table 2.** Identified vaporized products in gas and condensate fractions (Wt. % calculated to
823 the initial amount of PC-TBBA in sample as given in Table S1).
824 **Table 3.** Vibrational assignment for peaks in raw samples (Silverstein et al., 1991).
825 **Table 4.** Total bromine quantities within fractions (calculated to initial amount of PC-
826 TBBA in each sample as shown in Table S1).
827

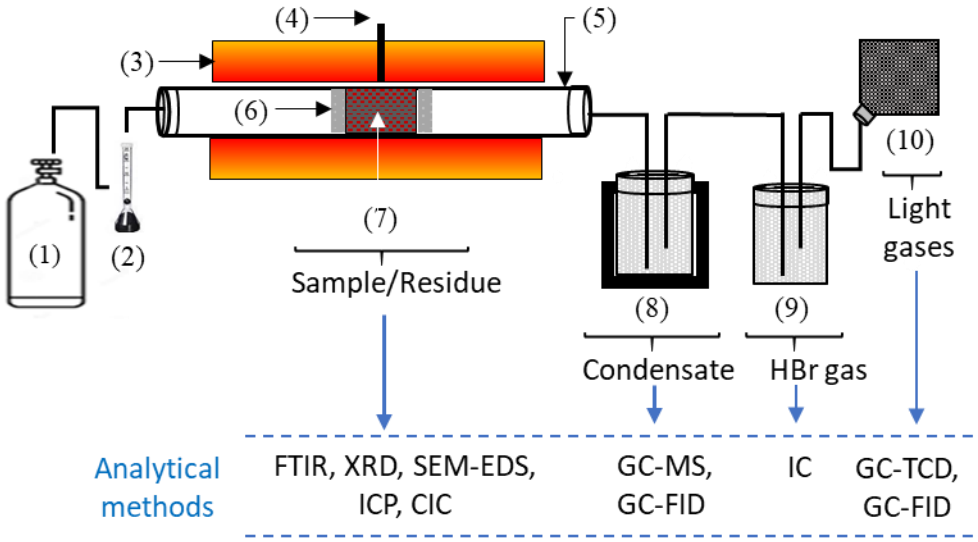

Fig. 1. Schematic diagram of the experimental set-up and overview of the analytical methods: (1) helium cylinder, (2) flow meter, (3) electric furnace, (4) thermocouple, (5) quartz tube reactor, (6) glass quartz wool, (7) sample/residue location, (8) liquid nitrogen-cooled condenser, (9) HBr trap in NaOH solution, (10) aluminum gas bag.

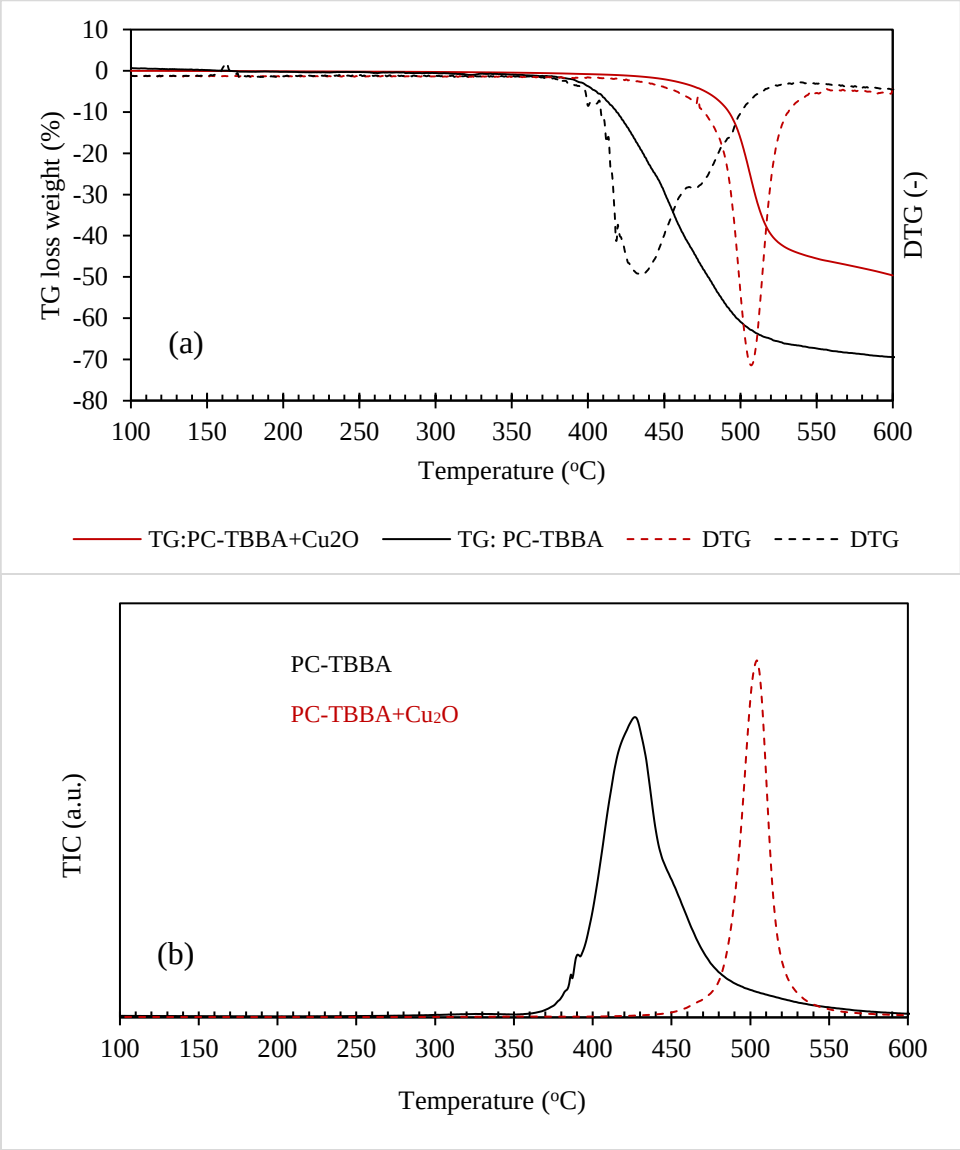

Fig. 2. TG and DTG curves (a), and TIC (b) for PC-TBBA and PC-TBBA+Cu_2O (3.8:1 *w/w*) under He flow.

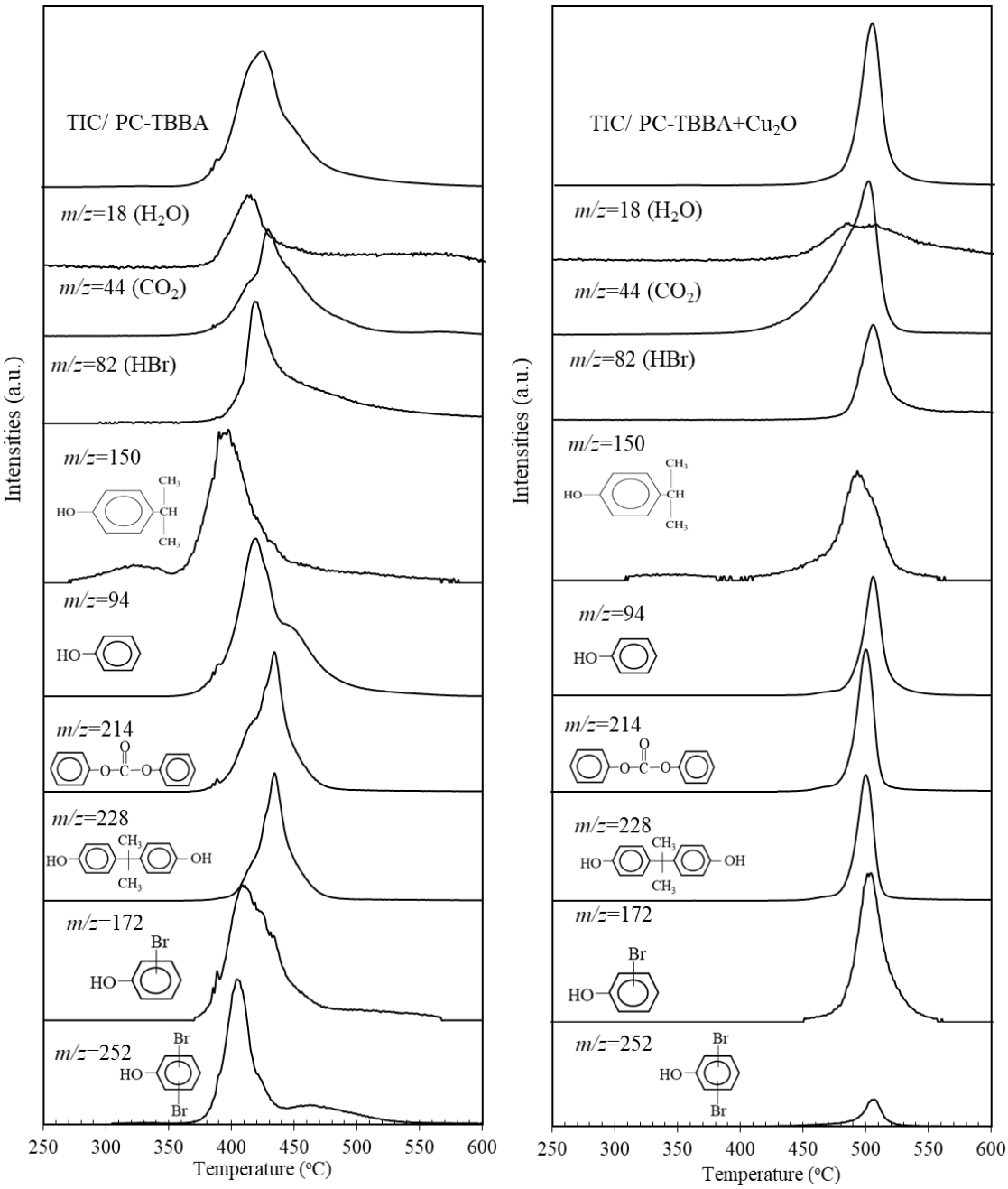

Fig. 3. Temperature dependent TIC and extracted ion chromatograms obtained from EGA-MS.

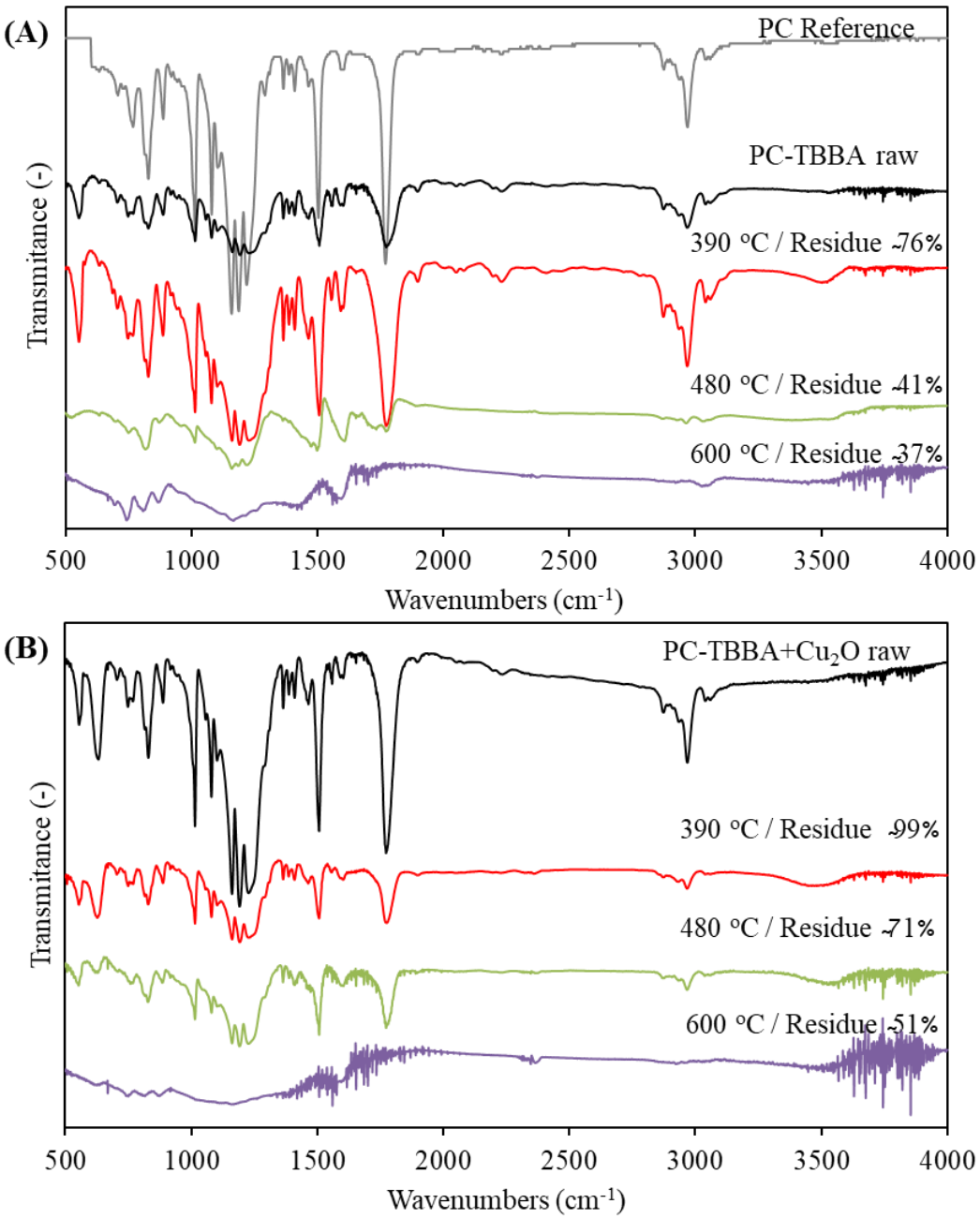

Fig. 4. Comparison of IR spectra of raw samples and residues from pyrolysis of PC-TBBA (A), and PC-TBBA+Cu_2O (B).

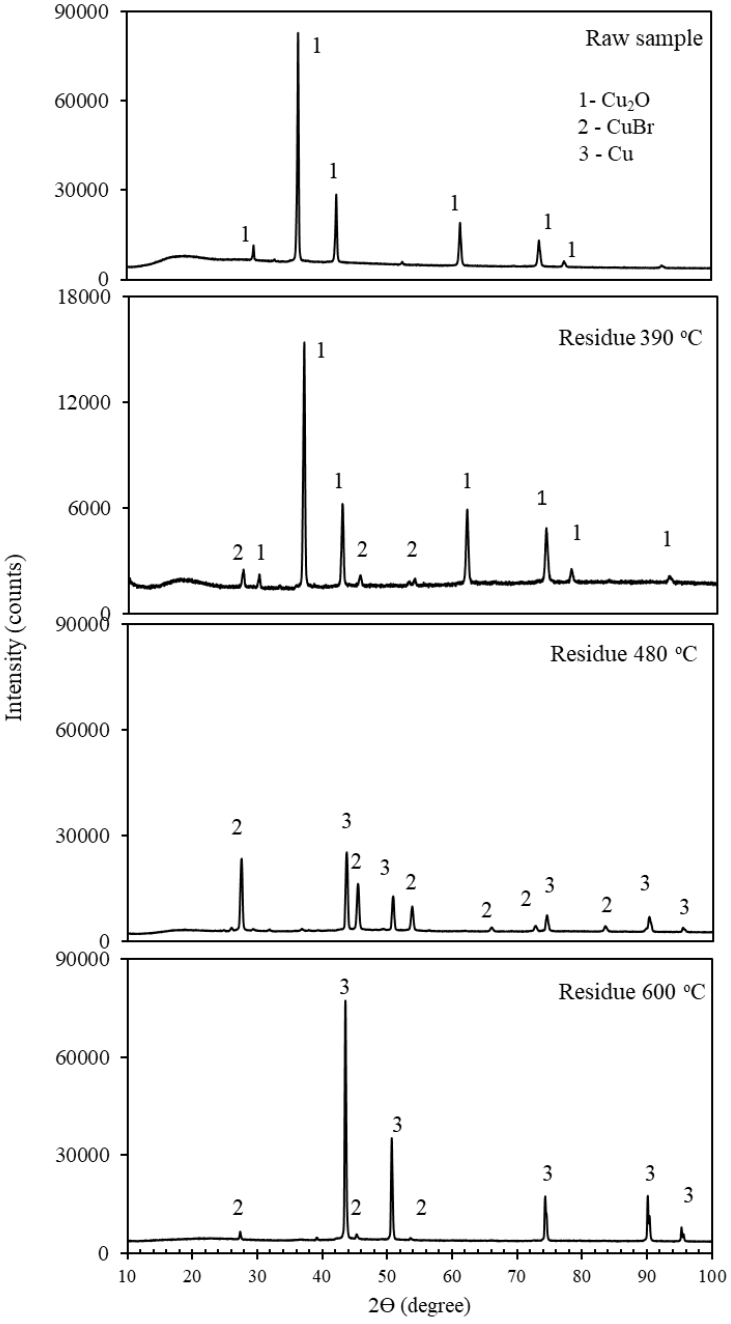

Fig. 5. XRD results of residues at various temperatures of pyrolysis of PC-TBBA+Cu_2O.

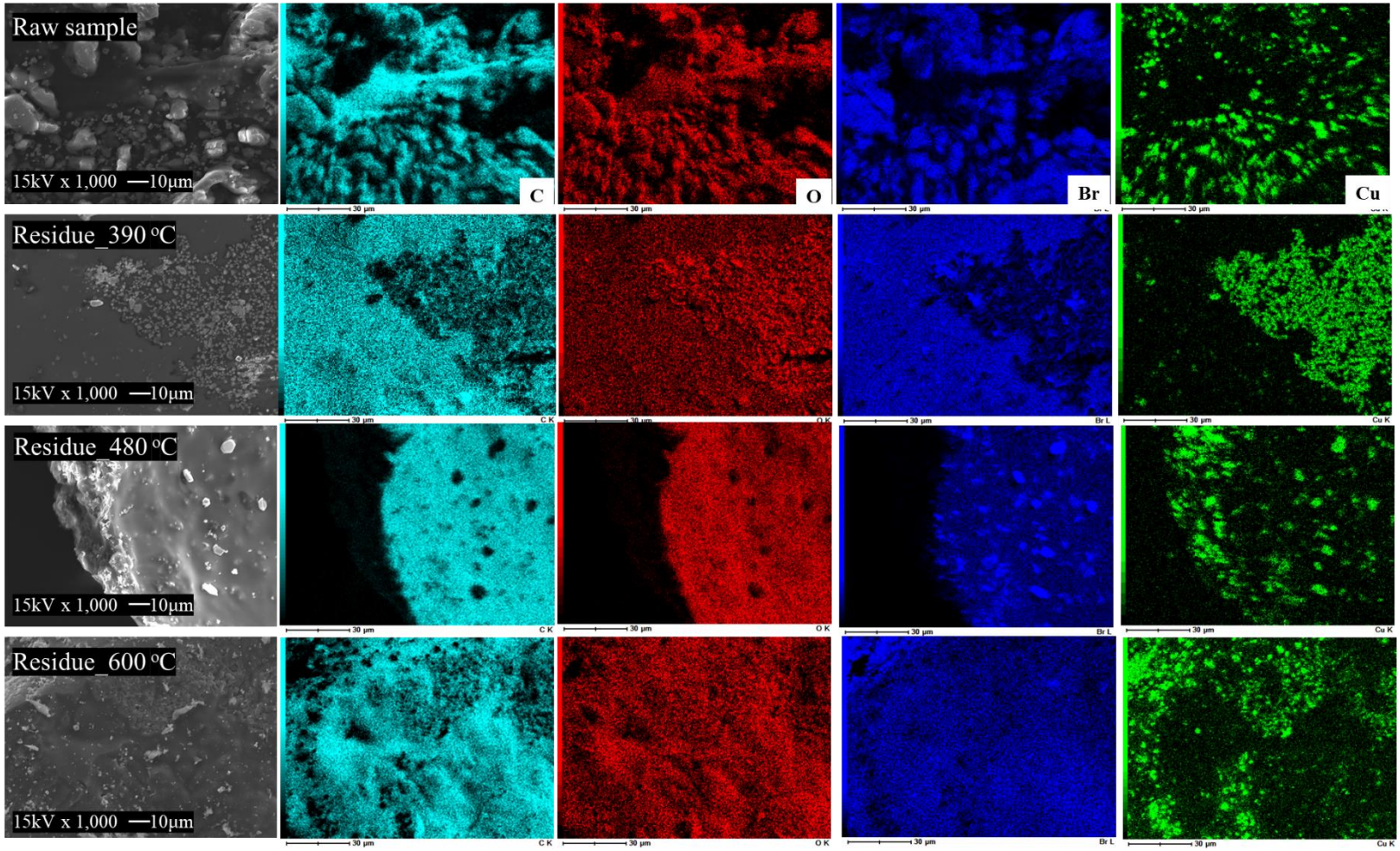

Fig. 6. SEM results of residues obtained at various temperatures of pyrolysis of PC-TBBA+Cu_2O.

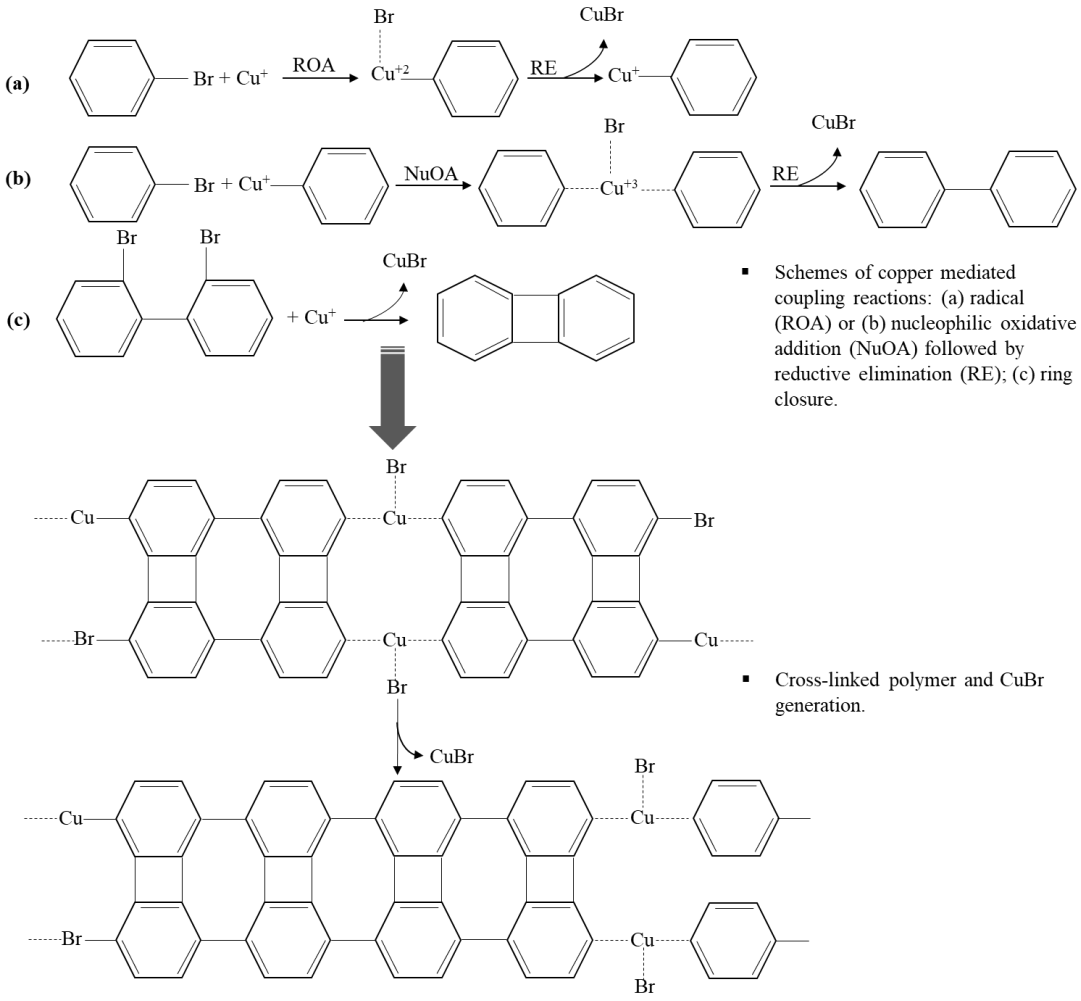

Fig. 7. Schemes of copper mediated coupling reactions generating cross-linking of polymer and CuBr.

Table 1. Composition of polycarbonate based tetrabromobisphenol A (PC-TBBA) and catalyst (Cu_2O) BET surface area characteristic.

Sample	Composition (w/w, %)					
	PC[a]	FR[a]	H[b]	O[b]	C[b]	Br[b]
PC-TBBA	>75%	<25%	4.7	18.4	65.0	11.8
Surface area characteristic by BET analysis[b]						
Catalyst	Surface area (m^2/g)		Total pore volume (cm^3/g)		Average pore diameter (nm)	
Cu_2O	0.7764		0.000381		1.9651	

[a)] Provided by supplier; [b)] Analyzed in this study; FR: Flame Retardant.

Table 2. Identified vaporized products in gas and condensate fractions (Wt. % calculated to the initial amount of PC-TBBA in sample as given in Table S1).

Name	Chemical structure	MW	PC-TBBA			PC-TBBA+Cu_2O		
			390 °C	480 °C	600 °C	390 °C	480 °C	600 °C
		(g/mol)	Wt. (%)					
Gas fraction ∑			***7.9***	***12.5***	***11.6***	***0.4***	***3.9***	***8.4***
Hydrogen bromide	HBr	81	6.5	7.4	7.5	0.3	0.3	1.2
Carbon monoxide	CO	28	1.2	3.1	3.6	n.d.	0.4	1.7
Carbon dioxide	CO_2	44	0.2	1.8	0.1	0.1	2.9	4.4
Methane	CH_4	16	n.d.	0.1	0.3	n.d.	0.4	1.0
Ethane	C_2H_6	30	n.d.	d.	d.	n.d.	d.	0.1
Propane	C_3H_8	44	n.d.	n.d.	n.d.	n.d.	n.d.	d.
Condensate fraction ∑			***14.8***	***48.9***	***53.8***	***1.4***	***21.0***	***44.6***
Phenols								
Phenol	C_6H_6O	94	3.1	8.4	11.4	n.d.	1.8	4.7
Phenol, 2-methyl-	C_7H_8O	108	d.	d.	0.1	d.	n.d.	0.1
Phenol, 4-methyl	C_7H_8O	108	d.	0.7	1.1	n.d.	0.6	3.0
Phenol, 4-ethyl-	$C_8H_{10}O$	122	d.	0.3	0.5	n.d.	0.4	1.2
p-Isopropylphenol	$C_9H_{12}O$	136	0.4	1.0	1.5	d.	0.4	0.8
p-Propylphenol	$C_9H_{12}O$	136	d.	d.	d.	n.d.	d.	0.1
p-tert-Butylphenol	$C_{10}H_{14}O$	150	0.5	0.5	0.5	d.	0.2	0.3
p-Isopropenylphenol	$C_9H_{10}O$	134	d.	0.2	0.1	n.d.	0.1	d.
2-Methyl-6-propylphenol	$C_{10}H_{14}O$	150	d.	d.	d.	n.d.	0.1	0.1
Phenol, 4-(1-methyl-1-phenylethyl)-	$C_{15}H_{16}O$	212	d.	0.5	0.5	n.d.	0.2	0.4
Phenol, 2,4`-isopropylidenedi-	$C_{15}H_{16}O_2$	228	0.2	d.	d.	n.d.	d.	d.
Phenol, 4,4`-(1-methyletylidene)bis-	$C_{15}H_{16}O_2$	228	0.2	7.6	7.9	d.	1.2	2.3

Phenol, 2-(1,1-dimethylethyl)-4-(1-methyl-1-phenyl	$C_{19}H_{24}O$	268	0.1	0.5	0.7	d.	d.	d.
Carbonyls								
Diphenyl carbonate	$C_{13}H_{10}O_3$	214	0.7	1.0	1.4	n.d.	d.	0.1
Carbonic acid, 4-methylphenyl phenyl ester	$C_{14}H_{12}O_3$	228	d.	d.	d.	n.d.	0.1	0.1
Ethers								
Diphenyl ether	$C_{12}H_{10}O$	170	d.	d.	d.	n.d.	d.	0.1
Benzene, 1-methyl-4-phenoxy-	$C_{13}H_{12}O$	184	d.	d.	d.	n.d.	d.	0.1
Benzene, 1-methyl-3-(4-methylphenoxy)-	$C_{14}H_{14}O$	182	d.	d.	0.1	n.d.	d.	0.1
Aromatics								
Biphenyl	$C_{12}H_{10}$	154	d.	d.	d.	n.d.	d.	d.
Dibenzofuran	$C_{12}H_8O$	168	d.	d.	d.	n.d.	d.	d.
3-Phenyl-benzofuran	$C_{14}H_{10}O$	194	d.	d.	d.	n.d.	d.	d.
Others								
3-Butene-1,2-diol	$C_4H_8O_2$	88	0.2	0.9	0.5	0.2	0.7	0.9
Butyrloacetone	$C_4H_6O_2$	86	3.4	2.4	2.1	n.d.	d.	d.
Brominated phenols								
2-Bromophenol	C_6H_5BrO	172	d.	0.3	0.2	n.d.	d.	0.1
4-Bromophenol	C_6H_5BrO	172	d.	0.3	0.4	n.d.	d.	0.1
2,4-Dibromophenol	$C_6H_4Br_2O$	250	1.0	1.0	1.2	n.d.	d.	d.
2,3,5-Tribromophenol	$C_6H_3Br_3O$	328	0.3	0.3	0.4	n.d.	0.1	0.1
2,6-Dibromo-4-(1,1-dimethylethyl)-phenol	$C_{10}H_{12}Br_2O$	306	d.	0.2	0.1	n.d.	d.	0.1
Brominated carbonyls								
Ethanone, 1-(3-bromo-4-hydroxyphenyl)-	$C_8H_7BrO_2$	214	d.	d.	0.1	n.d.	n.d.	0.1
Carbonic acid, p-bromophenyl phenyl ester	$C_{13}H_9BrO_3$	292	d.	0.1	0.1	n.d.	d.	d.
Brominated others								
1-Propanol-3-bromo	C_3H_7BrO	138	d.	0.1	0.1	d.	0.1	0.4
Unidentified compounds			4.9	22.7	23.0	1.1	14.9	28.9
Residue (organic fraction)			***76.4***	***41.2***	***36.9***	***99.3***	***71.2***	***50.8***

d. detected below 0.05 wt. %; n.d. not detected

Table 3. Vibrational assignment for peaks in raw samples (Silverstein et al., 1991).

Peak (cm^{-1})	Assignment	PC-TBBA	PC-TBBA+Cu_2O
3490-3530	Phenol O-H stretch	o	o
2968	CH_3 asymmetric stretch	o	o
2925	C-H stretch (alkyl)	o	o
1770	C=O stretch of carbonate group	o	o
1604	C-C bond ring stretch	o	o
1504	p-substituted ring stretch	o	o
1484	Asymmetric CH_3 deformation	o	o
1408	"Semicircle" ring stretch	o	o
1364	Symmetric CH_3 deformation	o	o
1188	$(CH_3)_2C=$ group	o	o
1160	-OCOO-	o	o
1080	Aromatic C-H and ring	o	o
1014	C-C in plane band	o	o
886	Sym. -OCOO- stretch	o	o
828	Aromatic C-H	o	o
768	-OCOO- and C-H deformation	o	o
630	Cu-O	x	o

Table 4. Total bromine quantities within fractions (calculated to initial amount of PC-TBBA in each sample as shown in Table S1).

Sample	Before experiment	After experiment		
	Br / solid[a]	Br / residue[a]	Br / condensate	Br / gas[b]
PC-TBBA	(mg)	(mg)		
390 °C	25.52	9.58	2.84	13.10
480 °C	25.82	0.50	10.22	15.10
600 °C	25.66	0.13 /0.5%	10.26/40%	15.20/60%
PC-TBBA+Cu_2O (3.8:1, w/w)				
390 °C	17.20	17.10 / 99.4	0.04	0.40
480 °C	17.21	15.98/ 93 %	0.73	0.50
600 °C	17.26	14.84 / 86%	0.52	1.90

[a)]Br determined by combustion ion chromatography (CIC); [b)]Br determined by IC; [c)]Br estimated from Eq. 1.

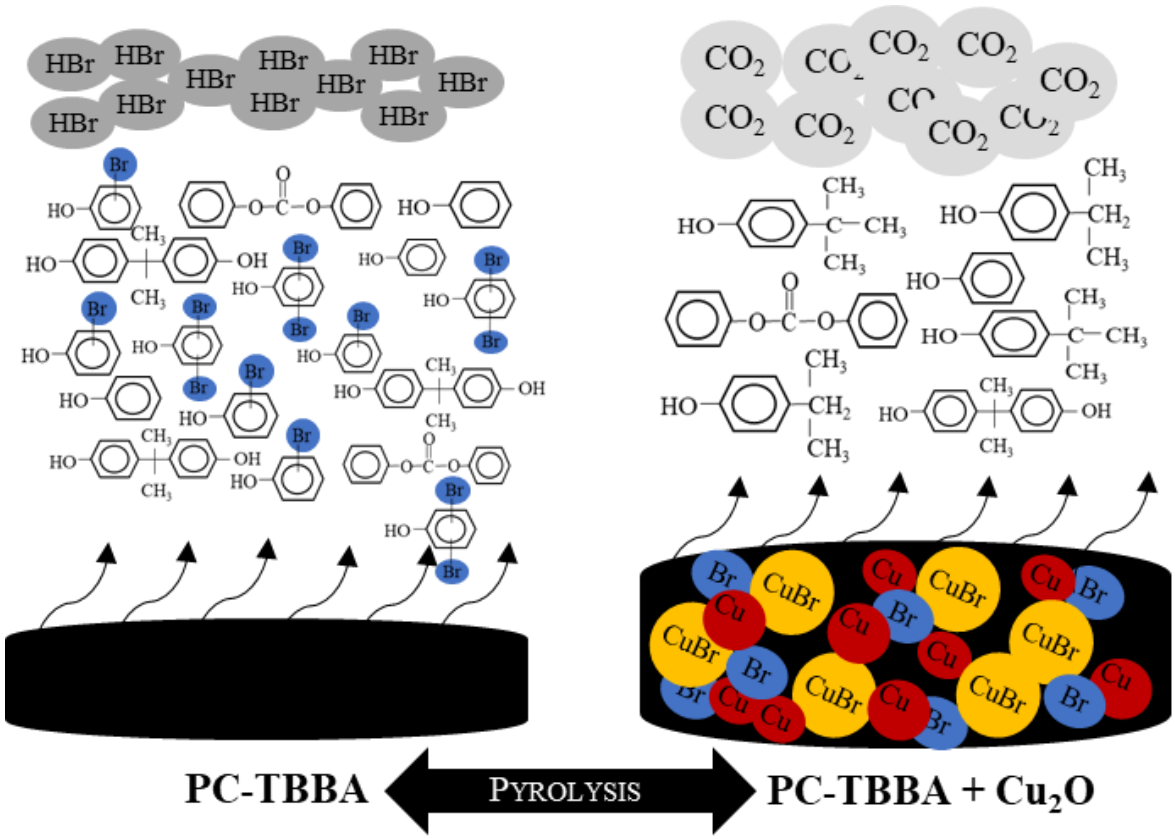
HBr
CO2
PC-TBBA
PYROLYSIS
PC-TBBA + Cu2O

Highlights

- Cu_2O significantly alter the pyrolysis of bromine-containing PC polymer.
- Cu_2O mediates cross-coupling of bromo-organics at early stage of pyrolysis.
- Cu_2O significantly reduces vaporization of bromo-organic products and HBr gas.
- Cu_2O utilizes efficiently CO in reduction reactions, favoring CO_2 generation.

Supplementary Table

Table S1. Mass balance for pyrolysis experiments.

Sample	Temp.	Sample weight before thermal treatment		Products weight after thermal treatment				Loss
		Sample		*Residue*		*Condensate*	*Gas*	
		Total[a]	Cu[b]	Total[a]	Cu[c]			
	(°C)	(g)	(g)	(g)	(g)	(g)	(g)	(g)
PC-TBBA	390	0.2006	-	0.1533	-	0.0297	0.0158	0.0018
	480	0.2030	-	0.0837	-	0.0992	0.0254	-0.0054
	600	0.2017	-	0.0745	-	0.1086	0.0234	-0.0048
PC-TBBA+Cu_2O (3.8:1 *w/w*)	390	0.2017	0.0399 ±0.0002	0.1984	0.0398	0.0022	0.0006	0.0005
	480	0.2018		0.1533	0.0396	0.0336	0.0063	0.0086
	600	0.2025		0.1215	0.0400	0.0715	0.0134	-0.0038

[a]"Total" refers to the total amount of PC-TBBA+Cu_2O before and after thermal treatment; [b]Cu values in raw mixture, analyzed twice; [c] Cu values analyzed once.

Supplementary Figures

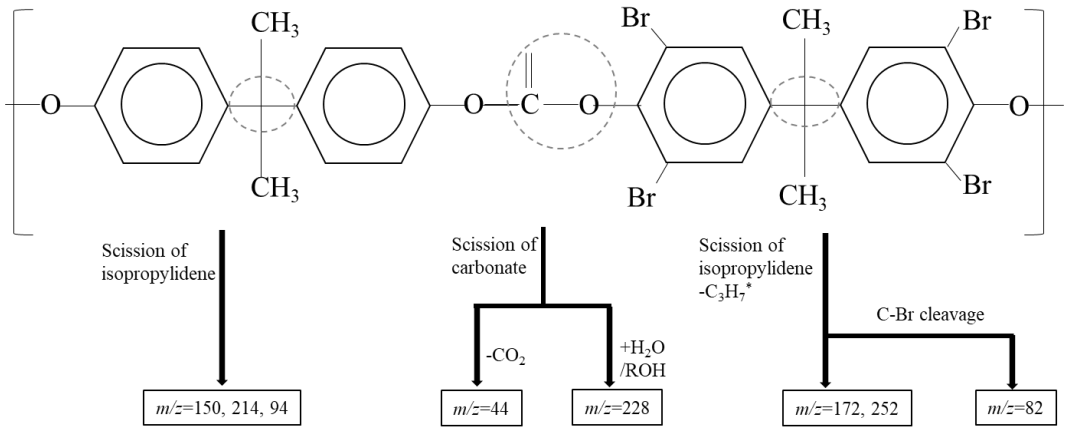

Fig. S1. Simplified initial pathways degradation based on thermal profiles from EGA-MS.

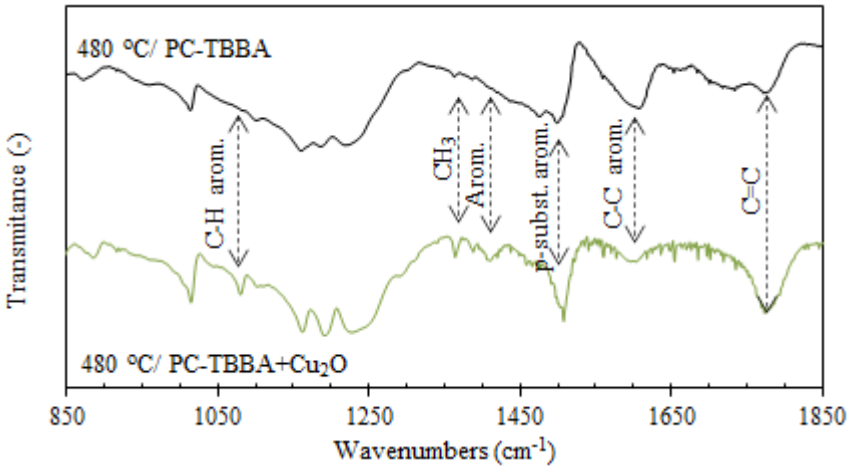

Fig. S2. Comparison of IR spectra of residues from pyrolysis of PC-TBBA, and PC-TBBA+Cu_2O at 480 ºC.